Early View publication on
www.wileyonlinelibrary.com
(issue and page numbers not yet assigned;
citable using Digital Object Identifier – **DOI**)

J. Biophotonics 1–19 (2012) / **DOI** 10.1002/jbio.201200015

Journal of
BIOPHOTONICS

REVIEW ARTICLE

Surface plasmon resonance based biosensor technique: A review

Xiaowei Guo[*,1,2]

[1] School of Electrical Engineering and Computer Science, and College of Engineering, Seoul National University, 599 Gwanangno, Gwanak-gu, Seoul 151-744, South Korea
[2] School of Optoelectronic and Information, University of Electronic Science and Technology, Chengdu, China, No. 4 sect. 2, North Jianshe road, Chengdu, 610054 China

Received 4 February 2012, revised 10 March 2012, accepted 11 March 2012
Published online 2 April 2012

Key words: Optical biosensor, surface plasmon resonance, microfluidics, optical fiber, nanoparticles

Optical Surface plasmon resonance (SPR) biosensors represent the most advanced and developed optical label-free biosensor technology. Optical SPR biosensors are a powerful detection and analysis tool that has vast applications in environmental protection, biotechnology, medical diagnostics, drug screening, food safety and security. This article reviews the recent development of SPR biosensor techniques, including bulk SPR and localized SPR (LSPR) biosensors, for detecting interactions between an analyte of interest in solution and a biomolecular recognition. The concepts of bulk and localized SPs and the working principles of both sensing techniques are introduced. Major sensing advances on biorecognition elements, measurement formats, and sensing platforms are presented. Finally, the discussions on both biosensor techniques as well as comparison of both SPR sensing techniques are made.

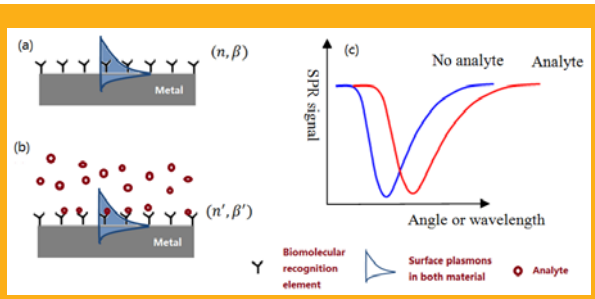

SPR biosensing principle: the analyte of interest is detected by measuring the change of the refractive index in the target solution.

1. Introduction

A biosensor is an analytical device for the analysis of biomaterial samples to gain an understanding of their bio-composition, structure and function by converting a biological response into an electrical signal [1]. It should basically consist of a transducer (electrochemical [2], piezoelectric [3], or optical [4]) and a recognition element which captures a specific analyte. In the past two decade, optical sensor development has been a fascinating and fast-paced area because they are immune to electromagnetic interference, capable of performing remote sensing, and can provide multiplexed detection within a single device. Various optical sensing methods have been exploited in biosensors including chemiluminescence [5, 6], fluorescence [7], light absorption and scattering [8, 9], reflectance [10], and SPR [11], which can be classified into two categories: label-based (the two formers) and label-free (the others). While

* e-mail: guosnu@gmail.com, Tel.: +82-02-3285-1738, Fax: +82-02-885-4459

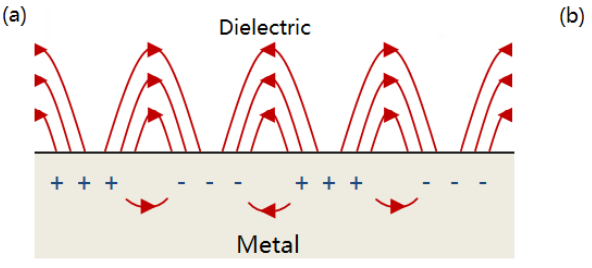

Figure 1 (online color at: www.biophotonics-journal.org) A SPR concept (**a**) and simulated SPs (**b**).

label-based detection is extremely sensitive, with the detection limit down to a single molecule [12], it suffers from laborious labeling processes that may also interfere with the function of a biomolecule. Quantitative analysis is challenging due to the fluorescence signal bias, as the number of fluorophores on each molecule cannot be precisely controlled [13]. In contrast, label-free detection behaves in their natural forms and relies on the measurement of binding-induced refractive index changes. As a result, this type of detection is relatively easy and cheap to perform, and allows for quantitative and kinetic measurement of molecular interactions.

In this review, we will focus on optical SPR biosensors because optical SPR biosensors have become a central tool for molecular interactions and provide a fast, specific and sensitive alternative to traditional laboratory analytical techniques. All the biosensors associated with SPR will be included in the review. While presenting this review, we note that there are several important reviews in the related areas [14–18]. Homola presented bulk SPR biosensors and summarized main application areas in chemical and biological species [16]. Another review concerns towards integrated SPR biosensors in which fiber and waveguide SPR biosensors are mentioned [17]. The LSPR biosensors were reviewed by Haes [18]. However, a comprehensive review for optical SPR sensors is absent. On the other side, recent advances in SPR biosensors need replenishments. Also, this review emphasizes on the sensing techniques rather than applications. The purpose of the present review tries to give out a clear understanding of SPR biosensor techniques.

To this end, we will start out from bulk and localized SPR concept, and then sensing principle. Based on the sensing principle, we will briefly but completely trace the technique advances in SPR biosensors. Finally we will provide the future scope of research and development of optic SPR biosensors.

2. Bulk SPR and localized SPR

SPs were widely recognized in the field of surface science following the pioneering work of Ritchie in the 1950s [19]. SPs are coherent electron oscillations that exist at the interface between any two materials where the real part of the dielectric function changes sign across the interface, typically on a metal-dielectric interface. These are essentially light waves that are trapped on the surface because of their interaction with the free electrons of the metal. In this interaction, the free electrons respond collectively by oscillating in resonance with the light wave. But the electron oscillations decay exponentially into both materials and the decay length is about wavelength order. The excitation of SPs by light is denoted as a bulk SPR or SPR in terms of conventional usage for planar surfaces (Figure 1) or LSPR for metallic nanoparticles (Figure 2) or metallic nanostructures, which are of interest to a wide spectrum of scientists, ranging from physicists, chemists and materials scientists to biologists [20, 21]. For researchers in the field of chemistry and biology, one of the most attractive aspects of SPs is the way in which these oscillations are very sensitive to any change of this boundary and therefore can be used as a sensing method for detection of external medium.

In bulk SPR case, the interaction between the surface charge density and the electromagnetic field results in the momentum of the SP mode, k_{SP}, being greater than that of a free-space photon of the same

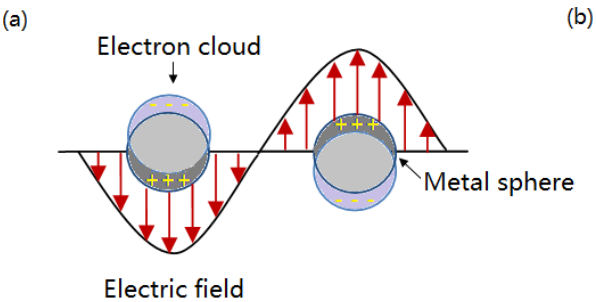

Figure 2 (online color at: www.biophotonics-journal.org) A LSPR concept (**a**) and simulated LSPs (**b**).

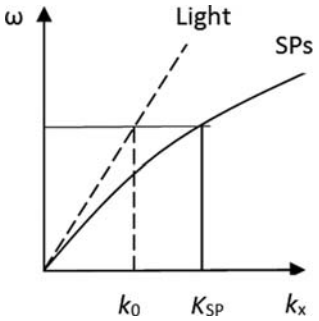

Figure 3 Dispersive curves for light in vacuum and SPs.

frequency, k_0, as shown in Figure 3. There are two main techniques by which the missing momentum can be provided. One is utilizing prism coupler to enhance the momentum of the incident light [22]. This method is referred to as the attenuated total reflection (ATR) method (Figure 4a). From ray optics viewpoint, use of waveguide or fiber structure to excite SPs is also based on the ATR method [23]. The dispersive relation of SPs can be expressed as below

$$k_{SP} = nk_0 \sin\theta \quad (1)$$

with n is the refractive index in incidence medium and θ is the incidence angle.

The other is based on a periodic corrugation in the metallic surface, typically metallic grating (Figure 4b) [24]. For one dimension grating, the dispersive relation of SPs can be written as

$$k_{SP} = k_x \pm mG \quad (2)$$

where k_x is the wave vector along the grating plane and its value is $nk_0 \sin\theta$, G is the reciprocal lattice vectors and m is integer. G equals to $2\pi/\Lambda$ and Λ is the pitch.

In LSPR case, the light scatters from a topological defect on the surface, such as a metallic nanostructures or nanoparticles, which provides a convenient way to generate LSPs [25]. Light interacts with metallic particles or nanostructures much smaller than the incident wavelength, which leads to a plasmon that oscillates locally around the nanoparticle

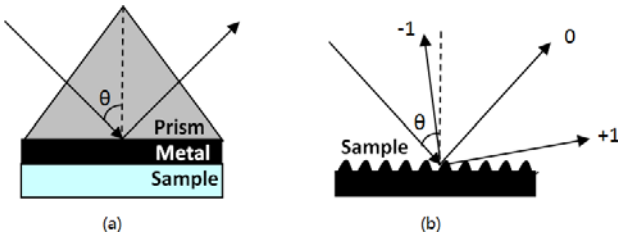

Figure 4 (online color at: www.biophotonics-journal.org) Excitation of SPs based on (**a**) a prism and (**b**) a grating coupler.

with a frequency. For noble spherical nanoparticles, e.g. Au or Ag, with diameters less than 30 nm, mainly dipole plasmon resonance is involved; however, for larger particles, quadrupole plasmon resonance from two negatively charged poles and two positively charged poles may be observed. The magnitude, peak wavelength and spectral bandwidth of the plasmon resonance associated with a nanoparticle are dependent on the particle's size, shape, and material composition, as well as its local dielectric environment.

3. Bulk SPR biosensors

Figure 5 shows the basic principle of an affinity SPR biosensor [15]. Biomolecular recognition elements on the surface of metal recognize and capture analyte present in a liquid sample producing a local increase in the refractive index at the metal surface. The refractive index increase gives rise to an increase in the propagation constant of SPs propagating along the metal surface which can be accurately measured by different optical means, such as intensity modulation, angular modulation, wavelength modulation, phase modulation, and even polarization modulation. The excitation of SPs at metal-dielectric interface results in the transfer of energy from incident photons to SPs. If the normalized reflection intensity is measured as a function of incident angle or wavelength by

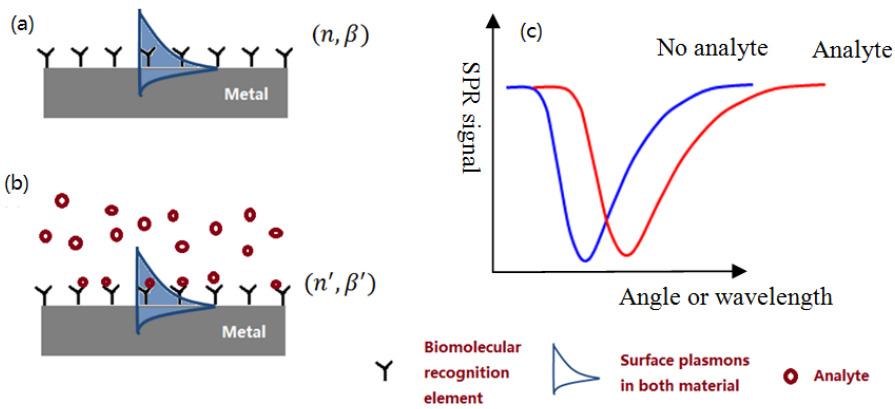

Figure 5 SPR biosensing principle. Biomolecular recognition elements on the surface of metal (**a**) recognize and capture analyte present in a liquid sample (**b**) producing a local increase in the refractive index at the metal surface. The refractive index increase induces a SPR signal shift (**c**).

keeping other parameters unchanged, then a sharp dip is observed at resonance angle or wavelength. For sensor applications, the refractive index change of a thin layer in contact with the metal surface of the sensor is monitored by measuring the spectral shift of the resonance dip (Figure 5c).

The first suggestion of SPR for biosensor purposes was 1983 [27]. Liedberg et al. demonstrated the potential of SPR based on prism coupler for immunology. In their experiments, a He-Ne laser was used for probe light and detected by a simple recorder. The antigen or antibody has simply been adsorbed to the metal surface prior to measurement. For example, Human IgG was adsorbed to the metal surface and then the solution of anti-IgG was injected into the cell. Anti-IgG binding to IgG resulted in a 0.3° shift of the resonance angle. Since that, SPR biosensors have made vast advances in terms of both development of the technology and its applications [14–16, 28, 29]. A large number of papers have been published using SPR for various analytical studies in such areas environmental protection, biotechnology, medical diagnostics, drug screening, food safety and security. A detailed summarization of the applications is given in Homola's 2008 review [16]. The following section is dedicated to the technique advances in SPR biosensors.

3.1 Advances in biorecognition elements

Various types of biorecognition elements and immobilization methods are available to allow biosensor platforms to be tailored for specific detection, mainly including antibodies, peptides and aptamers [30].

Antibodies are large Y-shaped proteins used by the immune system to identify and neutralize foreign objects such as bacteria and viruses. Antibody recognition elements make use of the sensitivity and specificity of bimolecular antibody-antigen interactions. The major advantage of antibody sensor biorecognition elements is that the immunogen need not be purified prior to detection. Besides conventional polyclonal and monoclonal antibodies, recombinant antibodies consisting of genetically manipulated fused antigen binding domains of common antibodies are another source for biosensor [31]. A number of recombinant antibodies have been shown to be useful for detection and identification of HIV, Hepatitis B and C, Simian immunodeficiency, Ebola, Rabies, Epstein–Barr, and Measles viruses as well as biological agents such as botulinum neurotoxin A/B [32, 33]. The early immobilization of protein on the gold surface is mainly via physical adsorption or electrostatic interactions, which may undergo conformational changes or adsorb with weak attachment [27]. The stable immobilization of proteins is via a covalent bond formed on the sensor surface through accessible functional groups of exposed amino acids e.g., lysine (amine group), cysteine (thiol group), with suitable types of derivatized surfaces, e.g. carboxylic acid, aldehyde, maleimide, vinyl sulfone [34, 35]. However, chemical binding via side chains of amino acids is often random, since it is based upon residues typically present on the exterior of the protein. In order to ensure that all the biomolecules are oriented in such a way that their binding sites are exposed to the sample solution, uniform alignment onto the surface should be achieved. Different site-specific immobilization techniques, e.g., Diels-Alder cycloaddition [36], "click" chemistry [37], peptide ligation [38], have therefore been presented in recent years. Another approach for site specific immobilization is based on biochemical affinity reaction, e.g. biotin-avidin/streptavidin reaction [39], histidine-chelated metal ion interaction [40] or DNA hybridization [41]. This approach provides not only oriented and homogeneous attachment, but possible to detach proteins and make repeated use of the same surface.

Peptides are short polymers of amino acid monomers linked by peptide bonds. In comparison with antibodies, peptides have been less used. In SPR biosensors, peptides have been applied mainly for the study of protein structure and function, e.g., antibodies against hepatitis G, herpes simplex virus, and Epstein-Barr virus [42–44]. They also were used for the detection of heavy metals and small ligand [45, 46]. Immobilization of peptides can follow strategies similar to those developed for proteins, including electrostatic attraction and amine- or thiol-based covalent coupling [45]. Small molecules with functional groups (aliphatic amines, thiols, aldehydes, or carboxylic groups) can be covalently linked to suitable corresponding groups on the sensor surface. Small molecules without suitable functional groups need to be derivatized [46]. Very recently, one step immobilization of peptides and proteins was reported through the covalent bonding of the formyl group with the primary amine groups of peptides and proteins [47].

The newly used one is aptamers. Aptamers are nucleic acid ligands (RNA, ssDNA, modified ssDNA, or modified RNA) that are isolated from libraries of oligonucleotides by an in vitro selection process called SELEX (Systematic Evolution of Ligands by Exponential enrichment) [48]. Since they are short, single-stranded oligonucleotides, they are capable of folding into three-dimensional structures due to their self-annealing properties. Although aptamers have been long applied as molecular recognition probes for a variety of sensor techniques such as electrochemical [49], piezoelectric [50], and optical sensors [51], SPR biosensors was rarely reported to use aptamers until 2001 [52]. This is due to the fact that the change in SPR signal resulting from the

binding process of aptamer with its target molecules is not very large. In recent years, aptamers are proposed as alternatives to antibodies as biorecognition elements in analytical devices with ever increasing frequency. Aptamers have been produced against a wide range of targets including drugs, proteins, and even supramolecular complexes such as viruses or bacteria [53–56]. The immobilization of aptamers (oligonucleotides) is often based on chemical bonding of the thiol group on gold surface. The most straightforward approach is to use biotinylated derivatives. The biotinylated aptamer is immobilized on the avidin or streptavidin layer through biotin-streptavidin interaction.

The ideal recognition surface should provide abundant immobilization sites and maintain the activity of the recognition element without initiating nonspecific interactions with other elements of the analytical media. There are lots of strategies for the construction of highly effective recognition surface [57]. To maximize the density of active surface groups, the technique of self-assembled monolayers (SAM), a kind of ordered molecular assemblies of different organic materials, was used to separate the immobilized molecules with a minimal distance [58]. For instance, SAM of thiols group is an effective chemical treatment to obtain highly ordered packed layer on the gold surface although the main drawback is nonspecific protein adsorption [59]. The use of this DNA SAM was expected to realize efficient hybridization because the ds portion can generate a space for hybridization and this method is expected to immobilize the probe portion on a substrate without DNA denaturation [60]. To reduce nonspecific absorption, poly/oligo (ethylene glycol) (PEG)-modified and peptide-based self-assembled monolayers have been developed. Ploy (carboxybetaine methacrylate) was also proven to be highly resistant to nonspecific absorption [61]. Peptide-based SAMs with complex biological media such as cell lysate and crude serum seems to be a powerful tool to minimize nonspecific absorption [62, 63], decreasing nonspecific adsorption to nearly 20–40 ng cm^{-2}, in contrast to commonly used PEG, which typically adsorbed 100 ng cm^{-2} of proteins. Another most commonly used method is to block the exposed surface with bovine serum albumin (BSA) [64, 65]. To provide more binding sites for capture molecules, three-dimensional matrices have been developed. The most widely used is carboxymethylated dextran provided by BioCore company in 1990 [66]. Agarose and aldehyde-agarose have been derivatized with primary amino groups and poly- (ethylenimine) to improve immobilization performances [67]. Hydrogels have the ability to hold water within the porous spaces available among the polymeric chains through which the capture molecules can diffuse, showing a 100-fold superior capacity of immobilization compared to that of planar surfaces [57].

3.2 Advances in measurement formats

Various measurement formats have been developed in SPR biosensor to ensure that the monitored binding event produces a measurable sensor response [68]. The most frequently used measurement formats are direct detection [69, 70], sandwich [71, 72], and competitive inhibition assay [73, 74].

Direct detection is usually preferred in applications where direct binding of analyte of concentrations of interest produces a sufficient response. In direct detection format, analyte in a sample interacts with a biomolecular recognition element immobilized on the sensor surface. The resulting refractive index change is directly proportional to the concentration of analyte. The lowest detection limits of the direct SPR biosensors can be improved by using sandwich assay and inhibit assay. In the sandwich assay format the measurement consists of two steps. Firstly, sample containing analyte is brought in contact with the sensor and the analyte molecules bind to the antibodies on the sensor surface. Then the sensor surface is incubated with a solution containing "secondary" antibodies. The secondary antibodies bind to the previously captured analyte further increasing the number of bound biomolecules and thus also the sensor response. However, the detection and quantification of low-molecular-weight analytes in the two formats is powerless. Competitive assay provides potential to detect smaller molecules. In this detection format, a sample is initially mixed with respective antibodies and then the mixture is brought in contact with the sensor surface coated with analyte molecules. The concentration of the antibody is kept constant so that the response variations are proportional to the amount of the analyte mixed with the antibody. An increase in the resonance angle occurs when the antibody binds with the conjugate immobilized on the surface. However, when an equilibrium mixture of antibody and analyte is allowed to flow over the conjugate, only the unbound antibody in the equilibrium mixture can be available for binding to the conjugate surface, and hence, a decrease in the resonance angle is observed. The measured binding response is, therefore, inversely proportional to the concentration of analyte in solution.

All the measurement efforts lead to a very limited change in SPR response. To increase the magnitude of the response, a second specifically interacting biomolecule is introduced as external label. Often this second molecule carries a high molecular weight or high refractive index tag. Consequently, a much larger change in SPR reflectivity can be observed. Liposomes [75], latex particles [76, 77], and certain proteins [78] have been tested as amplification tags. Following the idea, several kinds of metallic nano-

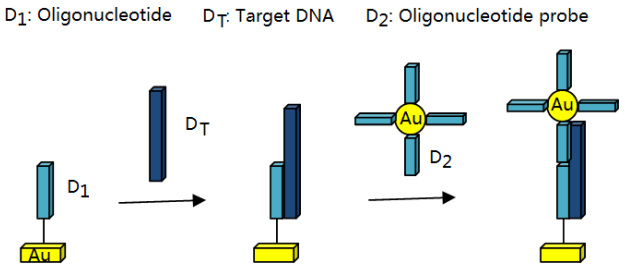

Figure 6 (online color at: www.biophotonics-journal.org) Gold nanoparticles to push the delect limit. Reprinted with permission from (95). Copyright (2007) American Chemical Society.

particles (NPs) including Au NPs, [79–83] Pd NPs, [84] and Pt NPs [85] had been applied to increase the SPR sensitivity for detecting all kinds of biomolecules, for example, the formation of antigen-antibody complexes, [86] DNA hybridization, [87] formation of aptamer-substrate complexes, [88] or enzymatic transformations [89]. Among them, Au NPs are most investigated in SPR biosensor due to its noble property which supports LSPR on particle surfaces. The strong coupling between the localized NP SPs and bulk SPs on the Au substrate results in a high sensitivity (Figure 6). Pollard-Knight et al. used 30 nm diameter colloidal Au nanoparticles in an immunoassay to demonstrate the concept of this amplification technique [90]. Natan group has developed an Au-amplified SPR sandwich immunoassay and achieved a pM detection of human immunoglobulin G [91], and conducted systematic studies of the effect of particle size and surface coverage on SPR response [92, 93]. He et al. demonstrated that use of the Au NP tags leads to a greater than 10-fold increase in angle shift in analysis of DNA hybridization, corresponding to a more than 1000-fold improvement in sensitivity for the target oligonucleotide as compared to the unamplified binding event [94]. In 2007, Wark et al. developed an ultrasensitive surface bioaffinity sensors for DNA hybridization by the adsorption of Au NPs onto gold diffraction gratings [95]. A limit of detect (LOD) 10 fM for DNA hybridization was obtained. In 2009, Wang et al. demonstrated the amplification effect of aptamer-Au NPs conjugates by using human immunoglobulin E as model analyte with a lowest LOD of 1 ng mL^{-1} [96]. In 2011, Gilad et al. created a multifunctional AuNPs which was functionalized with thiolated nucleic acid hairpin and implemented fM detection of DNA, adenosine monophosphate, and Hg^{2+} ions [97].

Recently, magnetic nanoparticle (MNP) labels have been also employed in SPR biosensorsto increase the binding-induced refractive index changes [98] and quick preconcentration and purification of target analytes in complex samples [99]. In 2010, Wang et al. presented an amplification technique using MNPs as external tags for an enhanced SPR bioassay [98]. Subsequently, Knoll group reported a SPR biosensor technology combining with use of external magnet to immobilize MNPs for detection and manipulating molecular analytes on the sensor surface [99]. The MNPs conjugated with antibodies specific to different analyte epitopes served both as labels for enhancing refractive index changes and as "vehicles" for the rapid delivery of analyte from a sample solution to the sensor surface. A lowest LOD of 0.45 pM was achieved.

3.3 Advances in sensing platforms

To increase the availability of analytes at a sensor's surface, SPR transducer is often used in conjunction with microfluidic flow channels, which allows use of small volumes of expensive reagents [100–102]. The typical progresses in sensing platforms were towards improvement of the sensor performance and multiple analyte analysis.

High sensitivity and resolution can be obtained by increasing the fraction of SPs in solution or the intensity of SPs at the sensor surface (Figure 7). For a thin metallic film sandwiched by two dielectric layers with a similar refractive index, there are two surface plasmon modes called long-range surface plasmon (LRSP) and short-range surface plasmon (SRSP), which are bound to both metal-dielectric interfaces [103]. The electric and magnetic fields of an

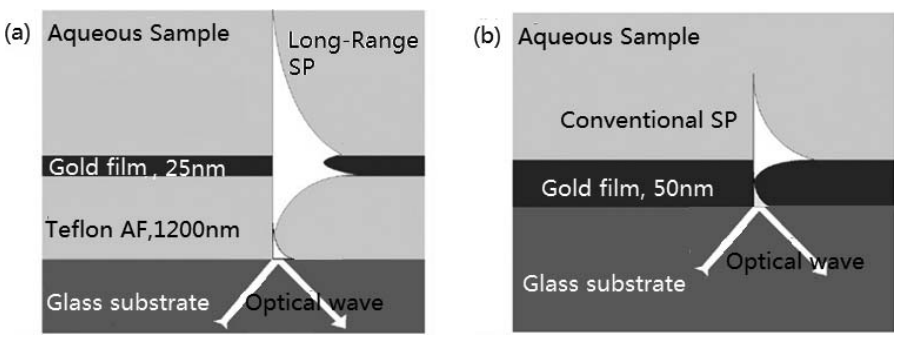

Figure 7 LRSP and Conventional SP. Reprinted with permission from (106). Copyright 2009, Elsevier.

LRSP are nearly perpendicular to the wave's direction of propagation with lateral confinement on the order of several wavelengths. Because of these characteristics, LRSPs can propagate the farthest of all known metallic modes, for instance, centimeter distances at infrared wavelengths and millimeters at visible wavelengths, making it suitable for large target molecules. The use of LRSPs was first proposed for sensing in 1990 by Matsubara et al. [104]. The use of LRSPs was shown to significantly improve both the sensor sensitivity and resolution. Nenninger et al. demonstrated an teflon-based LSPR biosensor capable of resolving refractive index changes as small as 3×10^{-7} RIU [105]. In 2007, Slavik et al. demonstrated an even better RI resolution of 3×10^{-8} RIU [106]. In 2011, Knoll group used LPSR-enhanced fluorescence spectroscopy for the detection of E. coli O157 : H7 [107]. The LOD below 10 cfu mL^{-1} was achieved. Generally, a silver film with a sharp SPR curve may yield a higher imaging sensitivity than a gold film since silver has a lower absorption of light [108]. However, the sensitivity of the SPR biosensor has a potential limitation, because silver is highly susceptible to oxidation. To prevent the oxidation of the sliver film, Choi et al. used garphene sheet on the sliver film [109] since the successful isolation of single atomic planes of graphite [110]. In particular, the graphene sheet is impermeable to gases as small as He atom [111]. This is attributed to the fact that the electron density of hexagonal rings is substantial enough to prevent atoms and molecules from passing through the ring structure [112]. The recent numerical study by Wu et al. demonstrated that a graphene-on-gold SPR biosensor can be more sensitive than the conventional gold film-based biosensors, due to the increased adsorption of target biomolecules on graphene [113]. Furthermore, use of spectroscopy of multiple SPs contributes to the improvement of the detection sensitivity. In 2006, Homola group reported an SPR sensor based on a special metallic grating with a profile composed of multiple harmonics [114]. A polychromatic light beam was made incident onto the grating, and the reflected light contained multiple SPR dips, one for each grating period. The use of multiple surface plasmons of different field profiles can provide more detailed information about the refractive index distribution at the sensor surface. It is also suggested to use a polychromatic light incident on a special diffraction grating acting as a SPR coupler and disperser (SPRCD) [115]. SPs was excited by the second order of diffraction. Simultaneously, the light diffracted into the first diffraction order was dispersed and the light components of different wavelengths were directed to different areas of a detector. The coupling of light into a surface plasmon resulted in a drop in the intensity of diffracted light, which was observed as a narrow dip in the spectrum of diffracted light. A refractive index resolution of this sensor was established at 3.5×10^{-7} RIU. In 2008, Guo et al. presented an SPR biosensor using both LRSP and SRSP excited simultaneously on a prism coupler with different angles [116]. This approach offers ability to distinguish sensor response caused by bulk and surface refractive index changes.

Many sensitive SPR biosensors are being presented but most of them only can detect one analyte. For practical applications, there is an urgent need for the development of SPR biosensors capable of multi-analyte detection. SPR sensors based on multichannel structures could provide a method for detecting multiple analytes simultaneously. In 1991, Sjolander et al. presented an integrated fluid flow system with three sensing channels on the surface of a glass prism [117]. A divergent beam produced by the LED was collimated and focused to produce a wedge-shaped beam of light hitting the glass-gold interface, which enables the use of multichannel monitoring. The reflected beams of light from the prism are collimated and projected onto the photodetector array. By immobilizing different sample amounts in different flowing channel, it is therefore possible to create multiple-step 'gradient' surface and thus make it easy for detection of low-molecular-weight analytes and for characterization of weak interactions [118]. The number of channels was later extended to 6 [119] and 10 [120]. An alternative way is to use multiple light beams irradiating parallel channels and the reflected signal is analyzed by multiple spectrographs [121]. There were two interesting parallel architectures with wavelength modulation. One is to deposit a dielectric overlayer over a part of the SPR-active surface [122]. The addition of the thin dielectric film shifts the coupling wavelength to a longer wavelength, the reflected light exhibits two dips associated with the excitation of surface plasmons in the area with and without the overlayer. The other approach is to use a special prism coupler with a tilted top surface [123]. The top surface reflects the incidence light onto different areas of the sensing surface at different angles of incidence. The surface plasmons on different regions are excited with different wavelengths which yielded an eight-channel SPR sensor with a resolution around 1×10^{-6} RIU. Multichannel sensors have been also realized using diffraction grating couplers [124]. In 2007, Jin et al. used a mirror as a light relay element and realized two fluidic grating channels for biomolecule binding [125]. In 2009, Partrik et al. reported a compact multichannel biosensor based on SPRCD diffraction grating-coupled SPR [126]. This approach provided potential to handle six independent sensing channels with temperature stabilization. A refractive index as low as 2×10^{-7} RIU was demonstrated to detect the binding of antibodies to the antigen-coated sensor surface. Zhang et al. also described a similar sensor

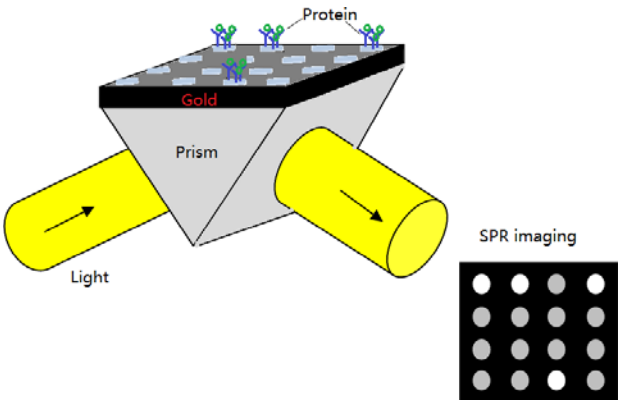

Figure 8 (online color at: www.biophotonics-journal.org) A SPRI biosensor.

chip with grating micro channels. Use of scanning method enables the SPR sensing with more channels [127].

The multichannel analysis described above is not suitable for high throughput detection. The SPR imaging (SPRI) technique is so far the most promising tool for high throughput detection [128]. The typical SPRI sensor is based on prism coupling (Figure 8), in which monochromatic incident light is expanded, passes through a prism and strikes the interface of the thin film and a prism at the coupling angle, exciting a broad area of the sensing surface. The reflected light is imaged on a CCD camera. Similar to the microarray technique, in SPRI the sensing chip is divided into many small sensing spots for detecting different analytes. Corn's group has been very active in the development and characterization of SPRI technique. They not only provided a wide variety of robust surface chemistries to link biological molecules (DNA, proteins, peptides, carbohydrates, RNA, etc.) to gold surfaces, and methods to deposit these in array formats appropriate for high-throughput applications using SPRI [129–135], but also demonstrated the application of DNA microarrays for SPRI-based detection of oligonucleotides [136] and ribosomal RNA [137], for monitoring the induced formation of hairpin structures [138], for studying the specific binding of two response regulators proteins to DNA [139], and the application of array-based detection with SPRI to quantitatively monitor carbohydrate-protein, peptide-protein, and protein–protein interactions, as well as surface enzyme kinetics [140–146]. It is highlighted that the enzyme chemistry enables SPRI technique to be an ultrasensitive platform. In 2011, they described a method where the specific sequence-dependent adsorption of a target ssDNA template molecule onto an ssDNA-modified gold microarray is followed with the generation of multiple copies of ssRNA via in situ surface transcription by RNA polymerase. This RNA transcription-based dual element amplification method is used to detect ssDNA down to a concentration of 1 fM [147]. Campbell's group demonstrated some applications of the method for absolute quantitative measurements to time- and spatially-resolved measurements of absolute coverages during protein binding onto gold and onto dsDNA microarrays on gold [148–150]. With a He–Ne laser as a source of light, their sensor was able to measure simultaneously in 120 sensing channels with a refractive index resolution of 2×10^{-5} RIU. In 2007, they improved the sensor resolution down to 5×10^{-6} RIU [151].

A lot of efforts have been devoted to the improvement of the SPRI sensing platform. Employing a highly coherent He–Ne laser as a source of illumination easily results in parasitic interference patterns that were disturbing SPR measurements, an incoherent light source with a NIR narrow band-pass filter was introduced [152]. Being highly sensitive, SPRI technique was affected by possible shape changes of the resonance which can be caused by unexpected modification of the surface roughness or by light absorbance. The diffracted or scattered light from the neighboring area around a sensing spot can also interfere with the radiation reflected from this spot. In 2005, Zybin et al. presented a dual-wavelength SPR imaging system [153]. The sensor output was defined as the difference of these two signals corresponding to two different wavelengths. A refractive index resolution of 2×10^{-6} RIU was achieved. Wavelength-tunable SPRI biosensors were reported by Nelson [154] and Fu [155]. Grating-based SPRI sensors have also been attracted many attentions because of their compatibility with mass production [156–158]. In 2001 Brockman et al. presented an SPRI grating device with an array of 400 sensing channels was prepared on the chip by means of spatially resolved fictionalization. In 2005, Homola's group used scanning method to obtain simultaneous measurements in over 200 sensing channels with a refractive index resolution of 5×10^{-6} RIU [157]. In 2008, they reported a two-dimensional SPRI sensor based on an array of metallic diffraction gratings. Each diffraction grating on a sensor chip serves both as an SPR coupler and a sensing channel. Parallel measurements with high-refractive index resolution of 5×10^{-7} RIU was achieved in 120 sensing channels [158]. Another research effort in SPRI is phase-sensitive SPR sensing, because the resonant phase behavior exhibits a steep jump, which leads to the potential in achieving extremely high sensitivity [159, 160]. In the earlier technique, a Mach-Zehnder interferometer with p-polarized as both signal and reference beams was used. Measurement sensitivity as good as 4×10^{-8} RIU was demonstrated with pure silver as the sensor surface [159]. In 2004, Wu. et al. presented a differential phase measurement technique by using p polarization as signal light and s po-

larization as reference light, which eliminates common-mode measurement fluctuations [161]. The SPR phase can be extracted by comparing the phase difference between the interference signals of p polarization and s polarization. In 2007, their experimental sensor resolution was 9.8×10^{-5} RIU [162]. Until now, SPR imaging in the phase domain has been mainly focused on analyzing the fringe pattern of interferograms [163, 164]. Spatial resolution over the sensor surface is limited and this makes it difficult to implement high-throughput microarray applications. Furthermore, phase detection is well known to be extremely sensitive to environmental vibration. Some of recent efforts focus on improvement of interrogation ability of SPRI instruments. To improve the addressability of individual spots, Luo et al. in 2008 designed two dimensional crossed-flow architecture with dedicated valves for each channel intersection to prevent cross-talk between horizontal or vertical channels [165]. While this approach added an additional level of control, entire microchannels were still exposed to the same analyte stream, limiting the number of interaction conditions. In 2010, Ouellet et al. developed an integrated microfluidic array for high-throughput SPRI-based detection and determination of binding affinities of antibodies against protein targets [166]. The device consists of 264 element-addressable chambers isolated by microvalves. The use of element-addressable chambers allows the interrogation of multiple ligand spots through multiple analyte streams, the device features a dilution network capable of simultaneous interrogation of up to six different analyte concentrations in a single experiment without the need for lengthy surface regeneration, and controlled recovery of rare samples is possible. Finally, the microfludic material on SPRI biosensors is being investigated. It is well known that PDMS devices perform poorly with the introduction of organic solvents into the channels, resulting in solvent leakage or swelling. An alternative material is necessary to develop organic-phase-based microfluidic devices. In 2011, Sheppard et al. presented Thiolene-based microfluidic devices have been coupled with SPRI to provide an integrated platform to study interfacial interactions in both aqueous and organic solutions [167].

4. Waveguide and fiber SPR biosensor

Most existing commercial SPR instruments rely on excitation of optical evanescent waves by prism-coupling of various designs. The prism-based instruments comprise several mechanical interfaces requiring a rather delicate mechanical system. In addition, since it is not practical to replace the whole prism when exchanging sensor surfaces, most of these instruments make use of index matching oils between a prism and an exchangeable glass plate with metal films. Such instruments therefore tend to suffer from mechanical wear and require extensive optical maintenance and technical service.

One technical route to overcome this challenge is based on integrating the light source, the prism and detector array in one disposable SPR sensor system [168–172]. For instance, a concept of the miniature SPR sensor is based on integration of all electro and optical components in a monolithic platform, Spreeta 2000 SPR sensor, developed by Texas Instruments in the mid-1990s [168]. Thirstrup et al. integrated the traditional prism and focusing optics in an injection moulded SPR sensor chip by means of diffractive optical coupling elements [173]. As an alternative, integrated SPR waveguide biosensors have been also investigated [174]. In 2001, Homola's group demonstrated that the SPR waveguide sensor was capable of measuring bulk refractive index changes smaller than 1.2×10^{-6} [175]. It consists of a channel waveguide locally covered with a metallic layer structure supporting surface plasmons. Light propagates through the waveguide and excites surface plasmons in the multilayer structure. In conjunction with specific bimolecular recognition elements, monoclonal antibodies, the sensor was capable of detecting 2 ng of hCG present in 1 ml of 1% bovine serum albumin solution. In 2004 another SPR waveguide biosensor with the capability of bipolarization wavelength interrogation was presented [176]. In the conventional SPR biosensors, only the transverse magnetic (TM)-polarized light wave can couple with the surface plasma wave. The proposed SPR biosensor can make both the TM- and the transverse electric (TE)-polarized light wave to produce the SPR. Therefore, two kinds of biomaterials can be separately detected by the signals from the TM- and the TE-polarized modes, and the number of detectable materials in a single chip can be doubled. Human serum albumin is coated on the device to sense the concentration of beta-blocker. Experimental results showed that the concentration of beta-blocker was related to the SPR wavelength shift at a rate of 0.08 and 0.027 nm/ppm for the TM- and the TE-polarized modes, respectively.

More convenient route is use of optical fiber as biosensor element that is very useful for remote sensing, point of care analysis and in situ monitoring. The development of optical fiber sensor can be dated back to the earlier 1990s. Jorgenson et al. replaced the traditional prism-based systems by a fiber optic design [177]. To generate SPs, they removed a segment of the cladding on a multimode fiber and coated a silver film around the exposed fiber core. In the meantime, Maria et al. used a fiber tip to excite SPs for microprobe [178]. After that, many types of optical fiber SPR sensors have been proposed in-

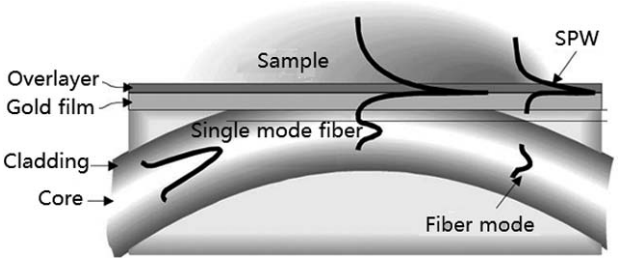

Figure 9 Side polished fiber SPR biosensor. Reprinted with permission from (190). Copyright 2001, Elsevier.

cluding side-polished or D-type [178–181], heterocore structure [182], tapered [183, 184], fiber grating [185–187], and metallic nanostructure or nanoparticles [188, 189]. Nevertheless, most of them were reported for chemical sensing purposes.

In 2001, R. Slavik et al. applied side-polished SPR fiber (Figure 9) for detection of IgG proteins via respective monoclonal antibodies immobilized on the SPR sensor surface [190]. The polished sensor surface was functionalized with a double-layer of anti-IgG molecules by glutaraldehyde. The depolarized light and spectral interrogation was used to overcome the limit of adverse sensitivity to fiber deformations. The sensor was operated using a flow injection system and mild acid was used to regenerate the surface for replicate analyses, and the sensor has been proved to be able to measure refractive index variations as small as 5×10^{-7}. In a continuation of this research, they used the same fiber optic SPR sensor for the detection of staphylococcal enterotoxin B [191]. The SPR biosensor was demonstrated to be able to detect ng mL^{-1} concentrations of SEB in less than 10 min. In 2009, Jang et al. combined the side-polished SPR fiber and the sandwich assay mode for the detection of prostate specific antigen [192]. The optical sensitivity of the SPR sensor was determined as 2.5×10^{-6} RIU. Pollet et al. used a SPR fiber biosensor for measuring DNA hybridization and DNA-protein interactions [193]. A fiber with a diameter of 400 μm and a numerical aperture of 0.39 allowed a specific incidence angle to excite SPs. A detection limit of 0.5 μM and 2 nM was observed for DNA hybridization and DNA-protein assays, respectively.

The methods mentioned above require total or partial removal of the fiber cladding or tapering down the fiber to allow core guided light to escape into the cladding, which excites the surface plasmons at the fiber core-metal layer interface. Therefore, one should carefully design and fabricate the SPR biosensors. These problems have resulted in a rise in cost. To overcome the disadvantages, fiber grating biosensors have been suggested [194–198, 200]. These fiber grating biosensors were realized by photo-writing a grating in fiber core which produces

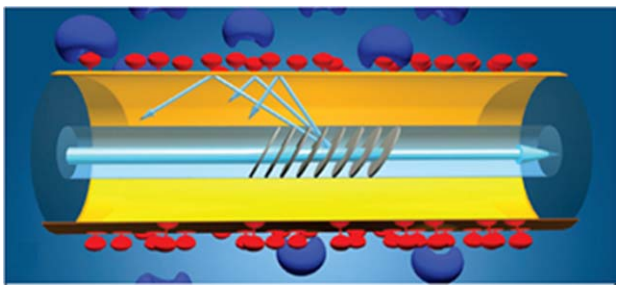

Figure 10 (online color at: www.biophotonics-journal.org) TFBG SPR biosensor. Reprinted with permission from (200). Copyright (2011) American Chemical Society.

a nonzero electric field in the cladding-sample interface. For example, long-period fiber gratings (LPFGs) couple light from the core mode to a forward-propagating cladding mode [196]. Short-period tilted fiber Bragg gratings (TFBGs) reflect the core field directly onto the cladding-sample interface through tilted grating surface [198], which is analogous to that in prism-based biosensors. By coating a metal layer on the fiber claddings, it was shown that it is possible to excite a particular cladding mode whose effective index is perturbed by a plasmon resonance of a metal coating on the fiber under the phase-matching conditions [199]. In 2006, Tang et al. presented a LPFG biosensor on which self-assembled gold colloids was coated [198]. The transmission spectra and optical properties of gold colloids change with the different refractive index of the environment near the surface of gold colloids. The sensor response of gold colloids increases linearly with solvents of increasing refractive index. When the colloidal gold surface was modified with a dinitrophenyl (DNP) compound, experimental results showed that the signal increase linearly with increasing concentration of the analyte, and the detection limit of the sensor for anti-DNP is 0.95 nM. In 2011, Y. Shevchenko et al. demonstrates that a TFBG-SPR sensor manufactured from an single mode fiber can be used as a biosensor to detect a bimolecular target at varying concentrations from 0.1 μM to 5 μM [200]. The TFBG biosensor is described in Figure 10. In their experiments, the thrombin aptamer immobilized on the surface of the sensor is used as a recognition element for binding of the thrombin protein. There is a unique advantage associated with the use of TFBG is the elimination of the effect of temperature cross-sensitivity from the sensor readings.

5. Localized SPR biosensors

The sensing principle of the LSPR method is based on the fact that the absorption and scattering spectra

of noble metal nanoparticles have a high sensitivity to the change of the nanoparticle shape [201, 202], size [203, 204], interparticle distance [205], dielectric properties of the nanoparticle material [206], and the dielectric properties of the surrounding medium [207–210]. Therefore, there are many tricks used for determining a sample concentration.

Gold and silver colloids display strong colors as a result of the plasmon absorption. This absorption is dependent on colloid-colloid proximity, which can be monitored by using UV-Vis spectroscopy. In 1996, Mirkin et al. made use of this simple concept to demonstrate DNA-directed assembly of colloidal gold as shown in Figure 11 [211]. In this work, two separate batches of 13nm-diameter gold nanoparticles were labeled with noncomplementary single-stranded thiol-capped DNA 8-mers. Upon adding a DNA duplex with eight base-pair-long 'sticky ends' that were complementary to each of the two prepared DNA/Au conjugates, colloidal assembly occurred, and the solution color changed as the nanoparticle electromagnetic coupling character increased. This assembly was reversible; by increasing the solution temperature above the DNA melting transition and then reducing it again, both the spectroscopic signal for DNA hybridization and that for nanoparticle aggregation cycled to reveal colloidal disassembly and reassembly. In related work, Elghanian et al. demonstrated that the nanoparticle/DNA/nanoparticle assembly time could be greatly shortened if the mixture was either heated to 50 °C or frozen in dry ice and isopropyl alcohol [212]. Even though the complete dissociation of the DNA strands (melting) is somewhat slow, as molecular associations weaken before duplex disassembly occurs, disassembly of the nanoparticle aggregate is quite fast, leading to sharp melting transitions when monitoring the LSPR. By considering both solution color changes and melting transition characteristics, it was possible to distinguish perfectly complementary target sequences from those that had single base pair mismatches, detecting as small as 10 fmol of oligonucleotide. The DNA duplex melting characteristics were further exploited by Nam et al. to distinguish antibody targets [213]. Specific oligonucleotide sequences were encoded onto the gold nanoparticles, and a complementary oligonucleotide modified with a biomolecule target binding partner was prehybridized to the nanoparticle-bound sequence. Upon introduction of the appropriate biomolecule target, the Au nanoparticles aggregate and a color change is seen. With judicious choice of the complementary oligonucleotide sequences, it was possible to control the melting behavior of the aggregated nanoparticles. Sequences with greater cytosine/guanine content have higher melting transitions. Accordingly, after a color change demonstrated that a biomolecule target was detected, a melting analysis revealed which target was detected. In 2001, the simple colorimetric technique was described for the detection of small concentrations of aqueous heavy metal ions, including toxic metals such as lead, cadmium, and mercury [214]. Functionalized gold nanoparticles are aggregated in solution in the presence of divalent metal ions by an ion-templated chelation process; this causes an easily measurable change in the absorption spectrum of the particles. The chelation/aggregation process is reversible via addition of a strong metal ion chelator.

Sensing based on scattering detections was reported in recent years [215–218]. In 2003, Roll et al. suggested the resonant Raleigh scattering detection approach for solution phase molecules using the light scattering properties of colloids with LED irradiation [215]. In this work, colloid aggregation was induced by avidin-biotin interactions, which shifted the plasmon absorption to longer wavelengths. It was found the spectral shift results in changes in the

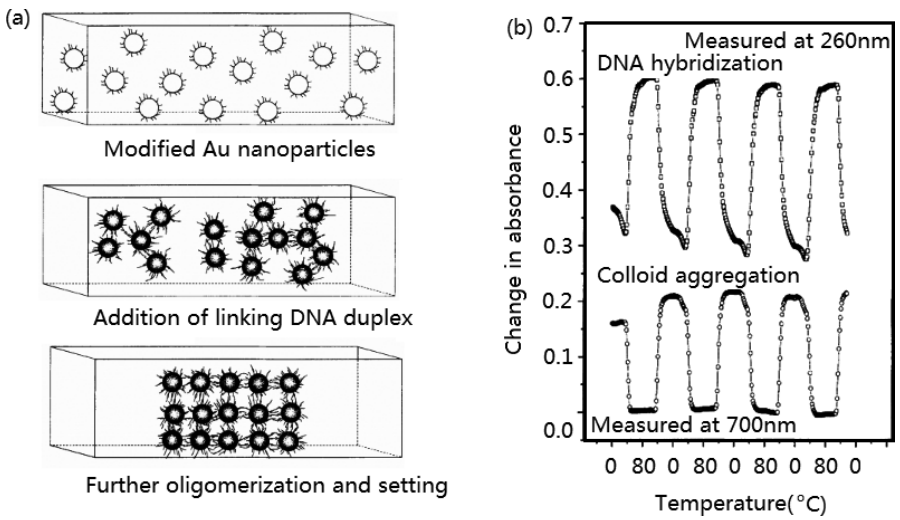

Figure 11 DNA-based colloide Au nanoparticle assembly (**a**) and Absorbance versus temperature profile for DNA/colloid hybridized materials (**b**). Reprinted with permission from (211). Copyright (1996) Nature Publishing Group.

scattering at different incident wavelengths. By measuring the ratio of scattered intensities at two incident wavelengths, this measurement was made independent of the total colloid concentration. The high scattering efficiency of the colloids resulted in intensities equivalent to fluorescence when normalized by the optical density of the fluorophore and colloid. In 2007, Mie scattering was used for spectroscopic study of the kinetic interaction between protein and gold nanoparticles [216]. The influence of the geometrical shape and size of the nanoparticles regarding the binding of a protein was investigated. Spherical nanoparticles of 60 and 100 nm diameters as well as ellipsoidal particles of dimension 20 by 60 nm for the minor and major axes respectively have been used. The nanoparticles were mounted in a quartz suprasil cuvette in a solution of millipore water. Light was incident on the cuvette and scattering by the particles was recorded by a monochromator. To each of the nanoparticle samples protein human serum albumin was added, and a series of spectra were immediately recorded to observe the expected shift in wavelength of the scattering maxima. By fitting the experimental data with theoretical predictions, the size of the nanoparticle and the distribution in the sample, the shape, the influence of sedimentation and the necessary kinetic parameters have been determined. Two-photon Rayleigh scattering (TPRS) [217–220] was used by Adria et al. in 2009 for detection of tau protein which plays a vital role in occurrence of Alzheimer's dementia in cerebrospinal fluid [217]. The TPRS approach is based on the fact that, the monoclonal ani-tau antibody-conjugated gold nanoparticles can readily and specifically identify Tau protein, through antibody–antigen interaction and recognition. For a Tau protein, there are many surface antigens available for specific recognition with monoclonal ani-tau antibody-conjugated nanoparticles. Therefore, in the presence of Tau protein, several nanoparticles can bind to each protein, thereby producing nanoparticle aggregates. As a result, a colorimetric change has been observed from red to bluish color and a new broad band appears around 150 nm far from their plasmon absorption band. This bioassay is rapid and takes less than 35 minutes from protein binding to detection and analysis and it can be three orders of magnitude more sensitive than the usual colorimetric technique. It have demonstrated two-photon scattering assay for the detection of Alzheimer's tau protein in 1 pg mL^{-1} level.

The disadvantage of aggregation-based colorimetric sensing technique is irreversible in most instances, and difficult to quantitate. An alternative method to circumvent the issue of irreversible complex formation is to synthesize nanoparticles bound to substrates [221–230]. In this method, these wavelength shifts are caused by adsorbate-induced local

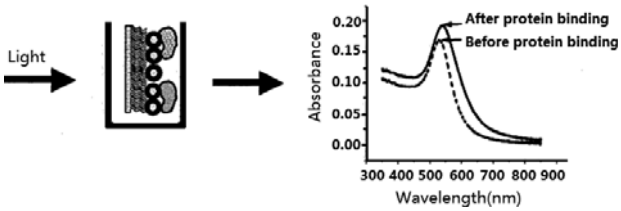

Figure 12 Biomolecular binding at the surface of the functionalized gold monolayer results in a absorption shift in peak wavelength. Reprinted with permission from (223). Copyright (2002) American Chemical Society.

refractive index changes shown in Figure 12. These nanoscale biosensors based on LSPR spectroscopy operate in a manner totally analogous to their SPR counterparts by transducing small changes in refractive index near the noble metal surface into a measurable wavelength shift response. In 2000, Okamoto et al. have demonstrated red-shifting of the LSPR band of gold nanoparticles immobilized on a glass substrate when the gold nanoparticles are coated with a dielectric layer several nanometers thick [221]. Himmelhaus et al. reported a highly sensitive biosensor using LSPR in cap-shaped gold nanoparticles immobilized on a dielectric substrate [222]. Nath et al. have also reported affinity biosensor using a glass substrate covered with gold nanoparticles, by measuring transmission absorption spectra [223, 224]. A solvent refractive index sensitivity of 76.4 nm RIU^{-1} and a detection of 16 nM streptavidin were achieved. Van Duyne group have exploited triangular silver nanoparticles based sensing techniques [226–231]. In 2002, a detailed study was presented demonstrating that triangular silver nanoparticles function as extremely sensitive and selective nanoscale affinity biosensors [227–229]. The biotin-streptavidin system was chosen to illustrate the attributes of these LSPR-based nanoscale affinity biosensors. Amplification of the LSPR nanobiosensor response was demonstrated using biotinylated Au colloids. In 2006, the effect of interacting molecular resonances and nanoparticle LSPRs was investigated [231]. It has been demonstrated that the LSPR peak shift and line shape induced by a resonant molecule vary with wavelength, and, in most instances, the oscillatory dependence of the peak shift on wavelength tracks with the wavelength dependence of the real part of the refractive index.

An effective method to improve the LOD of the LSPR sensing system is to reduce the number of nanoparticles probed. The method, however, requires a high sensitive detection instrument because the absorbance of a single nanoparticle is very close to the shot noise-governed LOD. In 2003, Van Duyne group has demonstrated that by using dark-field microscopy, single Ag nanoparticles can be used to sense local refractive index changes induced via bulk

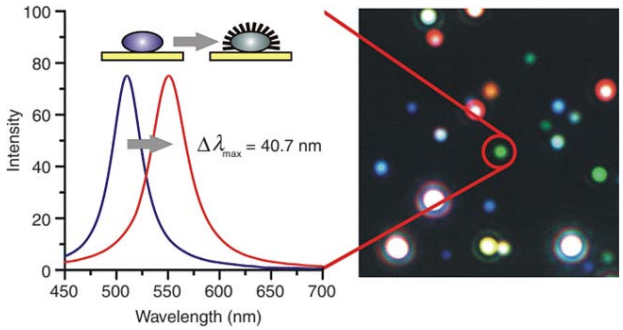

Figure 13 (online color at: www.biophotonics-journal.org) Single Ag nanoparticle biosensor. Reprinted with permission from (232). Copyright (2003) American Chemical Society.

solvent changes and a monolayer of alkanethiols [232]. In this work, a low density of chemically synthesized Ag nanoparticles was dispersed onto a clean glass coverslip. After recording the resonant Rayleigh scattering spectrum of an individual Ag nanoparticle in an N_2 environment, a 1.0 mM alkanethiol solution in ethanol was injected into the flow cell. After incubation in the analyte solution, the flow cell was flushed several times with ethanol, methanol, and hexane to ensure that a maximum of one monolayer had adsorbed. Finally, the nanoparticle was dried under N_2 and a scattering spectrum was recorded. The LSPR extinction maximum response of individual Ag nanoparticles to the adsorption of less than 60,000 hexadecanethiol molecules is about 40 nm (Figure 13). Using the same method, the detection of <100 streptavidin molecules per nanoparticle in a solution concentration of 1 pM by using nanoparticle array sensing was also demonstrated [233]. In 2010, the detection of a single molecule immunoassay was achieved using bipyramid gold nanoparticles by Mayer et al. Bipyramid gold nanoparticles have different LSPR spectrums from sphere nanoparticles [234]. Instead of monitoring antibody (Rabbit IgG)-antigen (Goat anti-Rabbit IgG) binding, they measured antibody-antigen unbinding events. The unbinding of single antigen molecule results in small, discrete <0.5 nm blue-shifts of the plasmon resonance.

6. Closing remarks and conclusions

Over the past two decade, optical SPR biosensors have achieved great advances which lead to many commercial SPR instruments. Most of them are based on prism coupling design, such as Biocore series (Biocore X to Biocore 4000), SR series (7000 and 7500), Autolab SPR, Plasmonic, Spreeta, Nanofilm, Multiskop. The Biocore series are the most famous and widely used SPR biosensors. For high throughput analysis, prism-based SPRI instruments such as SPRimagerII ARRAY (GWC Technologies), Lumera SPRI, IBIS SPRI, and SPRiLab (GenOptics), and Grating-based SPRI instruments such as BioRad's ProteOn XPR and Biacore's FlexChip, are available. Especially in the past few years, the performance of SPR biosensors increases quickly. The SPR and SPRI biosensors have been applied in molecular biology for the detection of proteins with a LOD ranging from picomolar to nanomolar [235–240], and detection of DNA molecules [130, 241–243] with the LOD as low as 54 fM with a flow injection device and as low as 1 fM when aided by signal amplification through gold nanoparticles [147, 244]. SPR also provides sensitive and fast detection of cancer biomarkers [245–248] and other biomarkers [249–251] with the LOD at ng mL^{-1} level for medical diagnosis. Additionally, SPR biosensors have been used for bacterial detection for environmental monitoring, food safety and homeland security with a LOD ranging from 10 to 106 cfu mL^{-1} [107, 252–254].

However, many challenges remain ahead. For an example, that ideal recognition surface is still not achieved. Many researchers suggest the range of SPR sensing applications is still hampered by the tricky issue of surface functionalization especially for array applications. Use of PEG or peptide or DNA SAM monolayer provides highly resistant to nonspecific absorption, but for SPR biosensor it can't offer enough reliable sensing signals. Three-dimension strategy provides more binding sites but simultaneously creates more chance for nonspecific absorption and thus results in high background signals. For another example, the LOD of the commercial SPR biosensors used in the fields of medical diagnosis and food safety is still low, typically in ng mL^{-1} level for most cases. For practical applications, further improvement is necessary. Au NPs conjugates and LRSPs provides possible solutions.

For optical fiber SPR biosensor, the sensitivity limit is usually around 10^{-5} to 10^{-6} RIU [175, 255]. Although the detection performance is far below that of prism-based SPR biosensors, it enables portable sensing and low cost. TFBG biosensor seems a promising tool to obtain high sensitivity, but there is a long way to go.

LSPR biosensor provides much lower sensitivity to changes in the bulk refractive index than SPR biosensor, but LSPR biosensors can be powerfully complementary to SPR biosensors. The response of the two techniques becomes comparable when measuring short-range changes in the refractive index owing to a molecular adsorption layer [256]. It is highlighted that single-nanoparticle LSPR spectroscopy is an option, offering ability to detect pM [233], even possible tens of fM sample concentration

[257]. The most pronounced advantage for LSPR biosensors is to provide promises for detection of single molecules although it is not evident now, which rivals that of conventional fluorescent label based biosensors.

Acknowledgements The work is supported by Brain Korea 21 project.

Xiaowei Guo received his B.S. degree in physics from Jinggangshan University, China, in 1998, and Ph.D. degree in physics from Sichuan University, China, in 2007. Then he joined the University of Electronic Science and Technology, China. From 2010 to 2011, he was a visiting scientist in MIT, USA. Currently, he is a BK21 postdoc researcher at the Seoul National University, Korea. He has published about thirty research articles. His areas of research are Micro/Nanophotonics, Micro/Nanofabrication, Microfluidics, and Biosensors.

References

[1] A. L. Ghindilis, P. Atanasov, M. Wilkins, and E. Wilkins, Biosens. Bioelectron. **13**, 113–131 (1998).
[2] X. Chu, Z. H. Lin, G. L. Shen, and R. Q. Yu, M. Analyst **120**, 2829–2832 (1995).
[3] P. Pless, K. Futschik, and E. Schopf, J. Food Prot. **57**, 369–376 (1994).
[4] G. Gauglitz, Sensor Update **1**, 1–48 (2001).
[5] W. C. W. Chan and S. M. Nie, Science **281**, 2016–2018 (1998).
[6] W. C. W. Chan, D. J. Maxell, X. H. Gao, R. E. Baily, M. Y. Han, and S. M. Nie, Curr. Opin. Biotechnol. **13**, 40–46 (2002).
[7] R. C. Mucic, J. J. Storhoff, C. A. Mirkin, and R. L. Letsinger, J. Amer. Chem. Soc. **120**, 12674–12675 (1998).
[8] M. D. Malinsky, K. L. Kelly, G. C. Schatz, and R. P. Van Duyne, J. Amer. Chem. Soc. **123**, 1471–1482 (2001).
[9] R. C. Mucic, J. J. Storhoff, C. A. Mirkin, and R. L. Letsinger, J. Am. Chem. Soc. **120**, 12674–12675 (1998).
[10] M. Mrksich, J. R. Grunwell, and G. M. Whitesides, J. Amer. Chem. Soc. **117**, 12009–12010 (1995).
[11] J. Homola, S. Yee, and G. Gauglitz, Sens. Actuators B **54**, 3–15 (1999).
[12] H. T. Li, L. M. Ying, J. J. Green, S. Balasubramanian, and D. Klenerman, Anal. Chem. **75**, 1664–1670 (2003).
[13] W. G. Cox and V. L. Singer, Biotechniques **36**, 114–122 (2004).
[14] J. Homola, S. Yee, and D. Myszka, Anal. Bioana. Chem. **377**, 528–539 (2003).
[15] J. Homola, Chem. Rev. **108**, 462–493 (2008).
[16] Robert Karlsson, J. molecular recognition **17**, 151–161 (2004).
[17] X. D. Hoa, A. G. Kirk, and M. Tabrizian, Biosens. Bioelectron. **23**, 151–160 (2007).
[18] J. A. Haes, P. Richard, and Van Duyne, Analyt. Bioanalyt. **379**, 920–930 (2004).
[19] R. H. Ritchie, Phys. Rev. **106**, 874–881 (1957).
[20] W. L Barnes, A. D. Thomas, and W. Ebbesen, Nature **424**, 824–830 (2003).
[21] K. A. Willets and R. P. Van Duyne, Annu. Rev. Phys. Chem. **58**, 267–297 (2007).
[22] E. Kretschmann and H. Raether, Z. Naturforsch. A **23**, 2135–2136 (1968).
[23] J. Arnaud, Opt. Quant. Electron. **12**, 3187–3191 (1980).
[24] R. H. Ritchie, E. T. Arakawa, J. J. Cowan, and R. N. Hamm, Phys. Rev. Lett. **21**, 1530–1533 (1968).
[25] E. Hutter and J. Fendler, Adv. Mater. **16**, 1685–1706 (2004).
[26] J. Homola, H. Vaisocherova, J. Dostalek, and M. Piliarik, Methods **37**, 26–36 (2005).
[27] B. Liedberg, C. Nylander, and I. Lundstrom, Sens. Actuators **4**, 299–304 (1983).
[28] J. Homola, Proc. SPIE **7503**, 75030P-1–75030P-6 (2009).
[29] J. Homola, in: Surface plasmon resonance (SPR) biosensors and their applications in food safety and security, in Frontiers in Planar Lightwave Circuit Technology: Design, Simulation, and Fabrication, S. Janz, J. Ctyroky, and S. Tanev (eds.) (Springer, 2006), pp. 101–118.
[30] P. J. Chambers, P. B. Arulanandam, L. L. Matta, A. Weis, and J. J. Valdes, Curr. Issues Mol. Biol. **10**, 1–12 (2008).
[31] P. A. Emanuel, J. Dang, J. S. Gebhardt, J. Aldrich, E. A. E. Garber, H. Kulaga, P. Stopa, J. J. Valdes, and A. Dion-Schultz, Biosens. Bioelectron. **14**, 751–759 (2000).
[32] M. J. O'Brien, V. H. Perez-Luna, S. R. Brueck, and G. P. Lopez, Biosens. Bioelectron. **16**, 97–108 (2001).
[33] V. A. Petrenko and I. B. Sorokulova, J. Mic. Meth. **58**, 147–168 (2004).
[34] V. Srivatsa, L. Rao, K. W. Anderson, and L. G. Bachas, Microchim. Acta. **128**, 127–143 (1998).
[35] D. J. Oshannessy, M. Brighamburke, and K. Peck, Anal. Biochem. **205**, 132–136 (1992).
[36] A. D. de Araffljo, J. M. Palomo, J. Cramer, M. Kohn, M. Schroder, R. Wacker, C. Niemeyer, K. Alexandrov, and H. Waldmann, Angew. Chem. **45**, 296–301 (2006).
[37] B. P. Duckworth, J. Xu, T. A. Taton, A. Guo, and M. D. Distefano, Bioconjugate Chem. **17**, 967–974 (2006).

[38] J. P. Tam, J. Xu, and K. D. Eom, Biopolymers **60**, 194–205 (2001).
[39] C. L. Smith, G. S. Milea, and G. H. Nguyen, Top. Curr. Chem. **261**, 63–90 (2006).
[40] S. Lata, A. Reichel, R. Brock, R. Tampe, and J. J. Piehler, Am. Chem. Soc. **127**, 10205–10215 (2005).
[41] C. M. Niemeyer, Trends Biotechnol. **20**, 395–401 (2002).
[42] N. Rojo, G. Ercilla, and I. Haro, Curr. Protein Pept. Sci. **4**, 291–298 (2003).
[43] C. Wittekindt, B. Fleckenstein, K. Wiesmuller, B. R. Eing, J. E. Kuhn, and J. Virol, Methods **87**, 133–144 (2000).
[44] H. Vaisocherova, K. Mrkvova, M. Piliarik, P. Jinoch, M. Steinbachova, and J. Homola, Biosens. Bioelectron. **22**, 1020–1026 (2007).
[45] E. S. Forzani, H. Q. Zhang, W. Chen, and N. J. Tao, EnViron. Sci. Technol. **39**, 1257–1262 (2005).
[46] O. R. Bolduc, P. L. Lanteigne, D. Y. Colin, S. S. Zhao, C. Proulx, D. Boeglin, W. D. Lubell, J. N. Pelletier, A. J. Fethiere, H. O. and J. F. Masson, Analyst. **136**, 3142–3148 (2011).
[47] H. Ko, E. H. Lee, G. Y. Lee, J. Kim, B. J. Jeon, M. H. Kim, and J. C. Pyun, Biosens Bioelectron. **30**, 56–60 (2011).
[48] A. D. Ellington and J. K. Szostak, Nature **346**, 818–822 (1990).
[49] K. Ikebukuro, C. Kiyohara, and K. Sode, Biosens. Bioelectron. **20**, 2168–2172 (2005).
[50] M. Liss, B. Petersen, H. Wolf, and E. Prohaska, Anal. Chem. **74**, 4488–4495 (2002).
[51] R. Yamamoto, T. Baba, and P. K. Kumar, Genes Cells **5**, 389–396 (2000).
[52] C. Nakamura, T. Kobayashi, M. Miyake, M. Shirai, and J. Miyakea, Mol. Cryst. Liq. Cryst. **371**, 369–374 (2001).
[53] H. Xiao, T. E. Edwards, and A. R. Ferre-DeAmare, Chem. Biol. **15**, 1125–1137 (2008).
[54] A. D. Keefe, S. Pai, and A. Ellingto, Nat. Rev. Drug Discovery **9**, 537–550 (2010).
[55] J. G. Bruno, M. P. Carrillo, T. Phillips, and C. J. Andrews, J. Fluoresc. **20**, 1211–1223 (2010).
[56] S. H. Jeon, B. Kayhan, T. Ben-Yedidia, and R. J. Arnon, Biol. Chem. **279**, 48410–48419 (2004).
[57] F. Rusmini, Z. Y. Zhong, and J. Feijen, Biomacromolecules **8**, 1775–1789 (2007).
[58] A. Ulman, Chem. Rev. **96**, 1533–1554 (1996).
[59] W. Knoll, M. Liley, D. Piscevic, J. Spinke, and M. J. Tarlov, Adv. Biophys. **34**, 231–250 (1997).
[60] Y. Sakao, F. Nakamura, N. Ueno, and M. Hara, Colloids Surf. B **40**, 149–152 (2005).
[61] R.G. Chapman, E. Ostuni, L. Yan, and G. M. Whitesides, Langmuir **16**, 6927–6936 (2000).
[62] O. R. Bolduc, C. M. Clouthier, J. N. Pelletier, and J. F. Masson, Anal. Chem. **81**, 6779–6788 (2009).
[63] O. R. Bolduc and J. F. Masson, Langmuir, **24**, 12085–12091 (2008).
[64] K. V. Gobi, H. Tanaka, Y. Shoyama, and N. Miura, Biosens. Bioelectron. **20**, 350–357 (2004).
[65] D. R. Shankaran, K. Matsumoto, K. Toko, and N. Miura, Sens. Actuators B **114**, 71–79 (2006).
[66] S. Lofas, B. Johnsson, A. Edstrom, A. Hansson, G. Lindquist, R. M. M. Hillgren, and L. Stigh, Biosens. Bioelectron. **10**, 813–822 (1995).
[67] S. Piletsky, E. Pletska, A. Bossi, N. Turner, and A. Turner, Biotechnol. Bioeng., **82**, 86–92 (2003).
[68] D. R. Shankaran, K. V. Gobi, and N. Miura, Sens. Actuators B **121**, 158–177 (2007).
[69] C. Nakamura, M. Hasegawa, N. Nakamura, and J. Miyake, Biosens. Bioelectron. **18**, 599–603 (2003).
[70] S. Sonezaki, S. Yagi, E. Ogawa, and A. Kondo, J. Imm. Methods **238**, 99–106 (2000).
[71] A. H. Severs, R. B. M. Schasfoort, and M. H. L. Salden, Biosens. Bioelectron. **8**, 185–189 (1993).
[72] J. Wei, Y. Mu, D. Song, X. Fang, X. Liu, L. Bu, H. Zhang, G. Zhang, J. Ding, W. Wang, Q. Jin, and G. Luo, Anal. Biochem. **321**, 209–216 (2003).
[73] N. Miura, K. Ogata, G. Sakai, T. Uda, and N. Yamazoe, Chem. Lett. **26**, 713–714 (1997).
[74] K. V. Gobi, H. Tanaka, Y. Shoyama, and N. Miura, Biosens. Bioelectron. **20**, 350–357 (2004).
[75] T. Wink, S. J. van Zuilen, A. Bult, and W. P. van Bennekom, Anal. Chem. **70**, 827–832 (1998).
[76] S. Kubitschko, J. Spinke, T. Bruckner, S. Pohl, and N. Oranth, Anal. Biochem. **253**, 112–122 (1997).
[77] E. F. A. de Vries, R. B. M. Schasfoort, J. van der Plas, and J. Greve, Biosens. Bioelectron. **9**, 509–514 (1994).
[78] C. E. Jordon, A. G. Frutos, A. J. Thiel, and R. M. Corn, Anal. Chem. **69**, 4939–4947 (1997).
[79] M. Riskin, R. Tel-Vered, O. Lioubashevski, and I. Willner, J. Am. Chem. Soc. **131**, 7368–7378 (2009).
[80] O. Lioubashevski, V. I. Chegel, F. Patolsky, E. Katz, and I. Willner, J. Am. Chem. Soc. **126**, 7133–7143 (2004).
[81] M. Zayats, S. P. Pogorelova, A. B. Kharitonov, O. Lioubashevski, E. Katz, and I. Willner, Chem. Eur. J. **9**, 6108–6114 (2003).
[82] J. L. Wang, A. Munir, and H. S. Zhou, Talanta **79**, 72–76 (2009).
[83] E. Golub, G. Pelossof, R. Freeman, H. Zhang, and I. Willner, Anal. Chem. **81**, 9291–9298 (2009).
[84] K. Q. Lin, Y. H. Lu, J. X. Chen, R. S. Zheng, P. Wang, and H. Ming, Opt. Exp. **16**, 18599–18604 (2008).
[85] D. Beccati, K. M. Halkes, G. D. Batema, G. Guillena, A. C. de Souza, G. van Koten, and J. P. Kamerling, Chem. Bio. Chem. **6**, 1196–1203 (2005).
[86] L. A. Lyon, M. D. Musick, and M. J. Natan, Anal. Chem. **70**, 5177–5183 (1998).
[87] L. He, M. D. Musick, S. R. Nicewarner, F. G. Salinas, S. J. Benkovic, M. J. Natan, and C. D. Keating, J. Am. Chem. Soc. **122**, 9071–9077 (2000).
[88] E. Golub, G. Pelossof, R. Freeman, H. Zhang, and I. Willner, Anal. Chem. **81**, 9291–9298 (2009).
[89] M. Zayats, S. P. Pogorelova, A. B. Kharitonov, O. Lioubashevski, E. Katz, and I. Willner, Chem. Eur. J. **9**, 6108–6114 (2003).
[90] D. P. Knight and C. R. Lowe, Biosens. Bioelectron. **8**, 355–363 (1993).
[91] L. A. Lyon, M. D. Musick, and M. J. Natan, Anal. Chem. **70**, 5177–5183 (1998).

[92] L. A. Lyon, M. D. Musick, P. C. Smith, B. D. Reiss, D. J. Pena, and M. J. Natan, Sens. Actuators, B **54**, 118–124 (1999).
[93] L. A. Lyon, D. J. Pena, and M. J. Natan, J. Phys. Chem. B **103**, 5826–5831 (1999).
[94] L. He, E. A. Smith, M. J. Natan, and C. D. Keating, J. Phys. Chem. B **108**, 10973–10980 (2004).
[95] A. W. Wark, H. J. Lee, A. J. Qavi, and R. M. Corn, Anal. Chem. **79**, 6697–6701 (2007).
[96] J. L. Wang, A. Munir, Z. H. Li, and H. S. Zhou, Biosens. Bioelectron. **25**, 124–129 (2009).
[97] G. Pelossof, R. T. Vered, X. Q. Liu, and I. Willner, Chem. Eur. J. **17**, 8904–8912 (2011).
[98] J. L. Wang, A. Munir, Z. H. Li, and H. S. Zhou, Anal. Chem. **82**, 6782–6789 (2010).
[99] Y. Wang, J. Dostalek, and W. Knoll, Anal. Chem. **83**, 6202–6207 (2011).
[100] M. Furuki, J. Kameoka, H. C. Craighead, and M. S. Isaacson, Sens. Actuators B **79**, 63–69 (2001).
[101] M. J. O'Brien, V. H. Perez-Luna, S. R. J. Brueck, and G. P. Lopez, Biosens. Bioelectron. **16**, 97–108 (2001).
[102] R. A. Vijayendran, K. M. Motsegood, D. J. Beebe, and D. E. Leckband, Langmuir **19**, 1824–1828 (2003).
[103] D. Sarid, Phys. Rev. Lett. **47**, 1927–1930 (1981).
[104] K. Matsubara, S. Kawata, and S. Minami, Opt. Lett. **15**, 75–77 (1990).
[105] G. G. Nenninger, P. Tobiska, J. Homola, and S. S. Yee, Sens. Actuators B **74**, 145–151 (2001).
[106] M. Vala, S. Etheridge, J. A. Roach, and J. Homola, Sens. Actuators B: Chem. **139**, 59–63 (2009).
[107] C. J. Huang, J. Dostalek, A. Sessitsch, and W. Knoll, Anal. Chem. **83**, 674–677 (2011).
[108] B. H. Ong, X. Yuan, S. C. Tjin, J. Zhang, and H. M. Ng. Sens. Actuators B. Chem. **114**, 1028–1034 (2006).
[109] S. H. Choi, Y. L. Kim, and K. M. Byun, Opt. Exp. **19**, 458–466 (2011).
[110] K. S. Novoselov, A. K. Geim, S. V. Morozov, D. Jiang, Y. Zhang, S. V. Dubonos, I. V. Grigorieva, and A. A. Firsov, Science **306**, 666–669 (2004).
[111] J. S. Bunch, S. S. Verbridge, J. S. Alden, A. M. van der Zande, J. M. Parpia, H. G. Craighead, and P. L. McEuen, Nano Lett. **8**, 2458–2462 (2008).
[112] D. E. Jiang, V. R. Cooper, and S. Dai, Nano Lett. **9**, 4019–4024 (2009).
[113] L. Wu, H. S. Chu, W. S. Koh, and E. P. Li, Opt. Exp. **18**, 14395–14400 (2010).
[114] P. Adam, J. Dostalek, and J. Homola, Sens. Actuators B **113**, 774–781 (2006).
[115] O. Telezhnikova and J. Homola, Opt. Lett. **31**, 3339–3341 (2006).
[116] J. Guo, P. Keathley, and J. Hastings, Opt. Lett. **33**, 512–514 (2008).
[117] S. Sjolander and C. Urbanitzky, Anal. Chem. **63**, 2338–2345 (1991).
[118] R. Karlsson and R. Stahlberg, Anal. Biochem. **228**, 274–280 (1995).
[119] M. J. O'Brien, V. H. Perez-Luna, S. R. J. Brueck, and G. P. Lopez, Biosens. Bioelectron. **16**, 97–108 (2001).
[120] R. Karlsson, J. Mol. Recogn. **17**, 151–161 (2004).
[121] H. C. Pedersen and C. Thirstrup, Appl. Opt. **43**, 1209–1215 (2004).
[122] J. Homola, H. B. B. Lu, G. G. Nenninger, J. Dostalek, and S. S. Yee, Sens. Actuators B **76**, 403–410 (2001).
[123] J. Dostalek, H. Vaisocherova, and J. Homola, Sens. Actuators B **108**, 758–764 (2005).
[124] C. R. Lawrence, N. J. Geddes, and D. N. Furlong, Biosens. Bioelectron. **11**, 389–400 (1996).
[125] Y. H. Jin and Y. H. Cho, in: Transducers and Eurosensors, Proc. 14th Inter. Conf. on Solid-State Sensors, Actuators and Microsystems, Lyon, France, 2007, pp. 811–814.
[126] M. Piliarik, K. Hegnerova, M. Vala, K. Chadt, I. Tichy, and J. Homola, Proc. SPIE **7192**, 719212-1–719212-9 (2009).
[127] N. Zhang, H. Liu, and W. Knoll, Biosens. Bioelectron. **24**, 1783–1787 (2009).
[128] C. Lausted, Z. Y. Hu, and L. Hood, Mol. Cell. Biochem. **7**, 2464–2474 (2008).
[129] E. A. Smith and R. M. Corn, Appl. Spectrosc. **57**, 320A–332A (2003).
[130] B. P. Nelson, T. E. Grimsrud, M. R. Liles, R. M. Goodman, and R. M. Corn, Anal. Chem. **73**, 1–7 (2001).
[131] J. M. Brockman, A. G. Frutos, and R. M. Corn, J. Am. Chem. Soc. **121**, 8044–8051 (1999).
[132] C. E. Jordan, A. G. Frutos, A. J. Thiel, and R. M. Corn, Anal. Chem. **69**, 4939–4947 (1997).
[133] H. J. Lee, Y. Li, A. W. Wark, and R. M. Corn, Anal. Chem. **77**, 5096–5100 (2005).
[134] H. J. Lee, A. W. Wark, Y. Li, and R. M. Corn, Anal. Chem. **77**, 7832–7837 (2005).
[135] T. T. Goodrich, H. J. Lee, and R. M. Corn, J. Am. Chem. Soc. **126**, 4086–4087 (2004).
[136] A. J. Thiel, A. G. Frutos, C. E. Jordan, R. M. Corn, and L. M. Smith, Anal. Chem. **69**, 4948–4956 (1997).
[137] B. P. Nelson, M. R. Liles, K. B. Frederick, R. M. Corn, and R. M. Goodman, Environ. Microbiol. **4**, 735–743 (2002).
[138] E. A. Smith, M. Kyo, H. Kumasawa, K. Nakatani, I. Saito, and R. M. Corn, J. Am. Chem. Soc. **124**, 6810–6811 (2002).
[139] E. A. Smith, M. G. Erickson, A. T. Ulijasz, B. Weisblum, and R. M. Corn, Langmuir **19**, 1486–1492 (2003).
[140] E. A. Smith, W. D. Thomas, L. L. Kiessling, and R. M. Corn, J. Am. Chem. Soc. **125**, 6140–6148 (2003).
[141] G. J. Wegner, H. J. Lee, and R. M. Corn, Anal. Chem. **74**, 5161–5168 (2002).
[142] S. Fang, H. J. Lee, A. W. Wark, H. M. Kim, and R. M. Corn, Anal. Chem. **77**, 6528–6534 (2005).
[143] H. J. Lee, A. W. Wark, and R. M. Corn, Langmuir **22**, 5241–5050 (2006).
[144] T. T. Goodrich, H. J. Lee, and R. M. Corn, Anal. Chem. **76**, 6173–6178 (2004).
[145] T. T. Goodrich, H. J. Lee, and R. M. Corn, J. Am. Chem. Soc. **126**, 4086–4087 (2004).
[146] H. J. Lee, Y. Li, A. W. Wark, and R. M. Corn, Anal. Chem. **77**, 5096–5100 (2005).

[147] E. I. Sendroiu, K. L. Gifford, A. Luptak, and M. R. Corn, J. Am. Chem. Soc. **133**, 4271–4273 (2011).
[148] J. S. Shumaker-Parry and C. T. Campbell, Anal. Chem. **76**, 907–917 (2004).
[149] J. S. Shumaker-Parry, R. Aebersold, and C. T. Campbell, Anal. Chem. **76**, 2071–2082 (2004).
[150] J. S. Shumaker-Parry, M. H. Zareie, R. Aebersold, and C. T. Campbell, Anal. Chem. **76**, 918–929 (2004).
[151] C. T. Campbell and G. Kim, Biomaterials **28**, 2380–2392 (2007).
[152] C. E. H. Berger, R. P. H. Kooyman, and J. Greve, Rev. Sci. Instrum. **65**, 2829–2836 (1994).
[153] A. Zybin, C. Grunwald, V. M. Mirsky, J. Kuhlmann, O. S. Wolfbeis, and K. Niemas, Anal. Chem. **77**, 2393–2399 (2005).
[154] B. P. Nelson, A. G. Frutos, J. M. Brockman, and R. M. Corn, Anal. Chem. **71**, 3928–3934 (1999).
[155] E. Fu, J. Foley, and P. Yager, Rev. Sci. Instrum. **74**, 3182–3184 (2003).
[156] J. M. Brockman and S. M. Fernandez, Am. Lab. **33**, 37–40 (2001).
[157] J. Dostalek, J. Homola, and M. Miler, Sens. Actuators B **107**, 154–161 (2005).
[158] J. Dostalek and J. Homola, Sens. Actuators B **129**, 303–310 (2008).
[159] S. G. Nelson, K. S. Johnston, and S. S. Yee, Sens. Actuators B **35**, 187–191 (1996).
[160] P. I. Nikitin, A. N. Grigorenko, A. A. Beloglazov, M. V. Valeiko, A. I. Savchuk, O. A. Savchuk, G. Steiner, C. Kuhne, A. Huebner, and R. Salzer, Sens. Actuators A **85**, 189–193 (2000).
[161] S. Y. Wu, H. P. Ho, W. C. Law, C. Lin, and S. K. Kong, Opt. Lett. **29**, 2378–2380 (2004).
[162] C. L. Wong, H. P. Ho, T. T. Yu, Y. K. Suen, Winnie W. Y. Chow, S. Y. Wu, W. C. Law, W. Yuan, W. J. Li, S. K. Kong, and Chinlon Lin, Applied optics, **46**, 2325–2332 (2007).
[163] Y. Xinglong, W. Dingxin, W. Xing, D. Xiang, L. Wei, and Z. Xinsheng, Sens. Actuators B **108**, 765–771 (2005).
[164] H. P. Ho and W. W. Lam, Sens. Actuators B **96**, 554–559 (2003).
[165] Y. Q. Luo, F. Yu and R. N. Zare, Lab Chip, **8**, 694–700 (2008).
[166] E. Ouellet, C. Lausted, T. Lin, C.Wei, T. Yang, L. Hood and E. T. Lagally, Lab Chip **10**, 581–588 (2010).
[167] G. Sheppard, T. Oseki, A. Baba, D. Patton, F. Kaneko, L. D. Mao, and J. Locklin, Biomicrofludics **5**, 026501–026506 (2011).
[168] J. Melendez, R. Carr, D. U. Bartholomew, K. Kukanskis, J. Elkind, S. Yee, C. Furlong, and R. Woodbury, Sens. Actuators B **35**, 212–216 (1996).
[169] J. L. Elkind, D. I. Stimpson, A. A. Strong, D. U. Bartholomew, and J. L. Melendez, Sens. Actuators B **54**, 182–190 (1999).
[170] T. M. Chinowsky, J. G. Quinn, D. U. Bartholomew, R. Kaiser, and J. L. Elkind, Sens. Actuators B **91**, 266–274 (2003).
[171] A. Naimushin, S. Soelberg, D. Bartholomew, J. Elkind, and C. Furlong, Sens. Actuators B **96**, 253–260 (2003).
[172] A. N. Naimushin, C. B. Spinelli, S. D. Soelberg, T. Mann, R. C. Stevens, T. Chinowsky, P. Kauffman, S. Yee, and C. E. Furlong, Sens. Actuators B **104**, 237–248 (2005).
[173] C. Thirstrupa, W. Zonga, M. Borrea, H. Neffad, H. C. Pedersenb, and G. Holzhueterc, Sens. Actuators B **100**, 298–308 (2004).
[174] J. Homola, J. Ctyroky, M. Skalsky, J. Hradilova, and P. Kolarova, Sens. Actuators B **38**, 286–290 (1997).
[175] J. Dostalek, J. Ctyroky, J. Homola, E. Brynda, M. Skalsky, P. Nekvindova, J. Spirkova, J. Skvor, and J. Schrofel, Sens. Actuators B **76**, 8–12 (2001).
[176] T. J. Wang, C. W. Tu, F. K. Liu, and H. L. Chen, IEEE Photon. Tech. Lett. **16**, 1715–1717 (2004).
[177] R. C. Jorgenson and S. S. Yee, Sens. Actuators B **12**, 213–220 (1993).
[178] L. D. Maria, M. Martinelli, and G. Vegetti, Sens. Actuators B **12**, 221–223 (1993).
[179] R. Alonso, F. Villuendas, J. Tornos, and J. Pelayo, Sens. Actuators A **37**, 187–192 (1993).
[180] A. Trouillet, C. Ronot-Trioli, C. Veillas, and H. Gagnaire, Pure Appl. Opt. **5**, 227–237 (1996).
[181] M. H. Chiu, S. F. Wang, and R. S. Chang, Opt. Lett., **30**, 233–235 (2005).
[182] P. C. Chiu, M. H. Chiu, M. C. Wang, Y. H. Kuo, C. G. Wang, M. T. Chen, and C. W. Yang, Proc. SPIE **6423**, 64232R/1–64232R/7 (2007).
[183] M. Iga, A. Seki, and K. Watanabe, Sens. Actuators B **101**, 368–372 (2004).
[184] A. Diez, M. V. Andres, and J. L. Cruz, Sens. Actuators B **73**, 95–99 (2001).
[185] Y. C. Kim, W. Peng, S. Banerji, and K. S. Booksh, Opt. Lett. **30**, 2218–2220 (2005).
[186] G. Nemova and R. Kashyap, Opt. Lett. **31**, 2118–2120 (2006).
[187] J. L. Tang, S. F. Cheng, W. T. Hsu, T. Y. Chiang, and L. K. Chau, Sens. Actuators B **119**, 105–109 (2006).
[188] N. Huy, G. W. Baxter, S. F. Collins, and A. Roberts, in: Proceedings of the 35th Australian Conference on optical fiber technology, December 2010, pp. 1–3.
[189] Y. Yanase, A. Araki, H. Suzuki, T. Tsutsui, T. Kimura, K. Okamoto, T. Nakatani, T. Hiragun, and M. Hide, Biosens Bioelectron. **25**, 1244–1247 (2010).
[190] R. Slavik, J. Homola, Jiri Ctyroky, and E. Brynda, Sens. Actuators B: Chem. **74**, 106–111 (2001).
[191] R. Slavik, J. Homola, and E. Brynda, Biosens. Bioelectron. **17**, 591–595 (2002).
[192] H. S. Jang, K. N. Park, C. D. Kang, J. P. Kim, S. J. Sim, and K. S. Lee, Opt, Comm. **282**, 2827–2830 (2009).
[193] J. Pollet, F. Delport, K. P. F. Janssen, K. Jans, G. Maes, H. Pfeiffer, M. Wevers, and J. Lammertyn, Biosens. Bioelectron. **25**, 864–869 (2009).
[194] M. Dagenais, A. N. Chryssis, S. M. Lee, H. Yi, S. S. Saini, and W. Bentley, Proc. SPIE, **5729**, 214–224 (2005).

[195] X. F. Chen, L. Zhang, K. M. Zhou, E. Davies, K. Sugden, I. Bennion, M. Hughes, and A. Hine, Opt. Lett. **32**, 2541–2543 (2007).
[196] S. Maguis, G. Laffont, P. Ferdinand, B. Carbonnier, K. Kham, T. Mekhalif, and M. Millot, Opt. Exp. **16**, 19049–19062 (2008).
[197] K. M. Guo, S. F. Cheng, L. K. Chau, and J. L. Tang, Optical Fiber Communication Conference, Optical Society of America, Anaheim, California, USA, 2005, pp. 1–3.
[198] J. L. Tang, S. F. Cheng, W. T. Hsu, T. Y. Chiang, and L. K. Chau, Sens. Actuators B **119**, 105–109 (2006).
[199] Y. Shevchenko and J. Albert, Opt. Lett. **32**, 211–213 (2007).
[200] Y. Shevchenko, T. J. Francis, D. A. D. Blair, R. Walsh, M. C. DeRosa, and J. Albert, Anal. Chem. **83**, 7027–7034 (2011).
[201] A. J. Haes, S. Zou, G. C. Schatz, and R. P. Van Duyne, J. Phys. Chem. B **108**, 109–116 (2004).
[202] A. J. Haes, S. Zou, G. C. Schatz, and R. P. Van Duyne, J. Phys. Chem. B **108**, 6961–6968 (2004).
[203] N. G. Khlebtsov, Anal. Chem. **80**, 6620–6625 (2008).
[204] X. Liu, M. Atwater, J. Wang, and Q. Huo, Colloids Surf. B **58**, 3–7 (2007).
[205] W. Rechberger, A. Hohenau, A. Leitner, J. R. Krenn, B. Lamprecht, and F. R. Aussenegg, Opt. Commun. **220**, 137–141 (2003).
[206] K. S. Lee and M. A. Elsayed, J. Phys. Chem. B **110**, 19220–19225 (2006).
[207] M. D. Malinsky, K. L. Kelly, G. C. Schatz, and R. P. Van Duyne, J. Amer. Chem. Soc. **123**, 1471–1482 (2001).
[208] J. J. Mock, D. R. Smith, and S. Schultz, Nano Lett. **3**, 485–491 (2003).
[209] W. A. Murray, B. Auguie, and W. L. Barnes, J. Phys. Chem. C **113**, 5120–5125 (2009).
[210] M. M. Miller and A. A. Lazarides, J. Phys. Chem. B **109**, 21556–21565 (2005).
[211] C. A. Mirkin, R. L. Letsinger, R. C. Mucic, and J. J. Storhoff, Nature **382**, 607–609 (1996).
[212] R. Elghanian, J. J. Storhoff, R. C. Mucic, R. L. Letsinger, and C. A. Mirkin, Science **277**, 1078–1081 (1997).
[213] J. M. Nam, S. J. Park, and C. A. Mirkin, J. Am. Chem. Soc. **124**, 3820–3821 (2002).
[214] Y. J. Kim, R. C. Johnson, and J. T. Hupp, Nano Lett. **1**, 165–167 (2001).
[215] D. Roll, J. Malicka, I. Gryczynski, Z. Gryczynski, and J. R. Lakowicz, Anal. Chem. **75**, 3440–3445 (2003).
[216] G. Doyle, B. Ashall, M. Galvin, M. Berndt, S. Crosbie, and D. Zerulla, Appl. Phys. A **89**, 351–355 (2007).
[217] A. Neely, C. Perry, B. Varisli, A. K. Singh, T. Arbneshi, D. Senapati, J. Rani Kalluri, and P. C. Ray, Nano. **3**, 2834–2840 (2009).
[218] R. W. Terhune, P. D. Maker, and C. M. Savage, Phys. Rev. Lett. **14**, 681–684 (1965).
[219] K. Clays and A. Persoons, Phys. Rev. Lett. **66**, 2980–2983 (1991).
[220] I. R. Antoine, E. Benichou, G. Bachelier, C. Jonin, and P. F. Brevet, J. Phys. Chem. C **111**, 9044–9048 (2007).
[221] T. Okamoto, I. Yamaguchi, and T. Kobayashi, Opt. Lett. **25**, 372–374 (2000).
[222] M. Himmelhaus and H. Takei, Sens. Actuators B **63**, 24–30 (2000).
[223] N. Nath and A. Chilkoti, Anal. Chem. **74**, 504–509 (2002).
[224] N. Nath and A. Chilkoti, Proc. SPIE **4626**, 441–448 (2002).
[225] S. Cheng and L. Chau, Anal. Chem. **75**, 16–21 (2003).
[226] C. L. Haynes and R. P. Van Duyne, J. Phys. Chem. B **105**, 5599–5611 (2001).
[227] M. D. Malinsky, K. L. Kelly, G. C. Schatz, and R. P. Van Duyne, J. Am. Chem. Soc. **123**, 1471–1482 (2001).
[228] A. J. Haes and R. P. Van Duyne, J. Am. Chem. Soc. **124**, 10596–10604 (2002).
[229] A. J. Haes and R. P. Van Duyne, Mat. Res. Soc. Symp. Proc. **723**, O3.1.1–O3.1.6 (2002).
[230] J. C. Riboh, A. J. Haes, A. D. McFarland, C. R. Yonzon, and R. P. Van Duyne, J. Phys. Chem. B **107**, 1772–1780 (2003).
[231] J. A. Haes, S. L. Zou, J. Zhao, C. G. Schatz, and P. R. Van Duyne, J. Am. Chem. Soc. **128**, 10905–10914 (2006).
[232] A. D. McFarland and R. P. Van Duyne, Nano Lett. **3**, 1057–1062 (2003).
[233] R. P. Van Duyne, A. J. Haes, and A. D. McFarland, Proc. SPIE **5223**, 197–207 (2003).
[234] K. M. Mayer, F. Hao, S. H. Lee, P. Nordlander and J. H. Hafner, Nanotechnol. **21**, 255503/1–255503/8 (2010).
[235] T. M. Chinowsky, M. S. Grow, K. S. Johnston, K. Nelson, T. Edwards, E. Fu, and P. Yager, Biosens. Bioelectron. **22**, 2208–2215 (2007).
[236] S. Tombelli, M. Minunni, E. Luzi, and M. Mascini, Bioelectrochem. **67**, 135–141 (2005).
[237] H. J. Lee, D. Nedelkov, and R. M. Corn, Anal. Chem. **78**, 6504–6510 (2006).
[238] W. C. Kuo, C. Chou, and H. T. Wu, Opt. Lett. **28**, 1329–1331 (2003).
[239] W. C. Law, P. Markowicz, K. T. Yong, I. Roy, A. Baev, S. Patskovsky, A. V. Kabashin, H. P. Ho, and P. N. Prasad, Biosens. Bioelectron. **23**, 627–632 (2007).
[240] T. M. Chinowsky, J. G. Quinn, D. U. Bartholomew, R. Kaiser, and J. L. Elkin, Sens. Actuators B Chem. **91**, 266–274 (2003).
[241] Y. J. Li, J. Xiang, and F. Zhou, Plasmonics **2**, 79–87 (2007).
[242] L. He, M. D. Musick, S. R. Nicewarner, F. G. Salinas, S. J. Benkovic, M. J. Natan, and C. D. Keating, J. Am. Chem. Soc. **122**, 9071–9077 (2000).
[243] F. Song, F. Zhou, J. Wang, N. Tao, J. Lin, R. L. Vellanowth, Y. Morquecho, and J. W. Laidman, Nucleic Acids Res. **30**, e72-1–e72-11 (2002).
[244] X. Yao, X. Li, F. Toledo, C. Z. Lopez, M. Gutova, J. Momand, and F. Zhou, Anal. Biochem. **354**, 220–228 (2006).

[245] G. A. Besselink, R. P. Kooyman, P. J. van Os, G. H. Engbers, and R. B. Schasfoorta, Anal. Biochem. **333**, 165–173 (2004).
[246] C. Cao, J. P. Kim, B. W. Kim, H. Chae, H. C. Yoon, S. S. Yang, and S. J. Sim, Biosens. Bioelectron. **21**, 2106–2113 (2006).
[247] J. W. Chung, R. Bernhardt, and J. C. Pyun, Sens. Actuators B Chem. **118**, 28–32 (2006).
[248] Y. Teramura and H. Iwata, Anal. Biochem. **365**, 201–207 (2007).
[249] J. Wei, Y. Mu, D. Song, X. Fang, X. Liu, L. Bu, H. Zhang, G. Zhang, J. Ding, W. Wang, Q. Jin, and G. Luo, Anal. Biochem. **321**, 209–216 (2003).
[250] J. F. Masson, L. Obando, S. Beaudoin, and K. Booksh, Talanta **62**, 865–870 (2004).
[251] M. Miyashita, T. Shimada, H. Miyagawa, and M. Akamatsu, Anal. Bioanal. Chem. **381**, 667–673 (2005).
[252] A. D. Taylor, Q. Yu, S. Chen, J. Homola, and S. Jiang, Sens. Actuators B Chem. **107**, 202–208 (2005).
[253] B. K. Oh, Y. K. Kim, K. W. Park, W. H. Lee, and J. W. Choi, Biosens. Bioelectron. **19**, 1497–1504 (2004).
[254] J. W. Waswa, C. Debroy, and J. Irudayaraj, J. Food Process Eng. **29**, 373–385 (2006).
[255] A. Suzuki, J. Kondoh, Y. Matsui, S. Shiokawa, and K. Suzuki, Sens. Actuators B Chem. **106**, 383–387 (2005).
[256] A. J. Haes and R. P. Van Duyne, Anal. Bioanal. Chem. **379**, 920–930 (2004).
[257] T. A. Taton, C. A. Mirkin, and R. L. Letsinger, Science **289**, 1757–1760 (2000).